PAPER

The critical role of hydrogen on the stability of oxy-hydroxyl defect clusters in uranium oxide†

Joseph M. Flitcroft, [a] Marco Molinari, *[ab] Nicholas A. Brincat,[c] Nicholas R. Williams,[c] Mark T. Storr,[c] Geoffrey C. Allen[d] and Stephen C. Parker *[a]

Despite considerable work applying *ab initio* techniques to model the role of defects on mechanical, structural and electronic properties of oxides, there has been little on the role of trapped hydrogen, despite it being virtually always present. We propose a framework for identifying reversible and irreversible hydrogen traps. We demonstrate that the thermodynamic stability of oxy–hydroxyl defects is defined by an interplay of formation and binding energies. This framework is applicable to all oxides and is essential for describing the solubility and diffusivity of hydrogen at the macroscopic level. For the most important actinide oxide in nuclear energy, uranium oxide, hydrogen significantly impacts the stability of oxygen defect clusters, and with increased local hydrogen concentration it forms irreversible traps. Crucially, hydrogen stabilises isolated Willis clusters, named after their discoverer and originally reported in 1963, which all subsequent *ab initio* calculations have predicted to be unstable, but of course, none considered hydrogen.

Introduction

The presence of hydrogen in oxide materials is often overlooked despite its significant impact on materials properties,[1–4] including mechanical resistivity,[5] conductivity,[6] (photo-)catalysis,[7–9] gate materials,[10] insulator to metal transition[11] and chemo- and photo-chromism.[12] Perhaps one of the most compelling arguments, for investigating hydrogen defects, is that control over these materials properties would only be gained when a complete survey of the chemistry and atom-level structures of complex defects is compiled.

Hydrogen is of primary concern in metals and uranium is no exception, with its legacy from the first generation of nuclear reactors. As a metal, uranium is susceptible to oxidation in the presence of water vapour and oxygen forming a thin uranium oxide coating layer that provides a protective physical barrier that quenches corrosion of the metal. In common with other metals,[5] the aqueous corrosion of uranium generates hydrogen species that permeate through the oxide layer[13–15] and react with the metal to form hydride species.[16] However, uranium hydride is pyrophoric and thus it is a major concern in the design of long-term storage facilities. To prevent formation of the hydride, trapping of hydrogen within the oxide coating layer is required, and this can be best achieved by identifying and controlling the defects that efficiently trap hydrogen.

In the case of uranium oxide, experimental data on solubility and diffusivity of hydrogen is limited,[17–19] and the nature of the diffusing hydrogen species is still undetermined, with both molecular[17] and atomic[18,19] hydrogen proposed. The latter, in particular, is essential for predicting any diffusivity and trapping. Evidence of hydrogen trapping was first reported by Sherman and Olander,[19] who saw the release of hydrogen from samples at high temperatures (800–1450 °C). Wheeler suggested that this hydrogen may be in the form of strongly bound species (*i.e.* hydroxyl groups) that are effectively trapped.[17]

There is also evidence that oxygen deficiency increases hydrogen solubility compared to oxygen-rich conditions.[19] In the latter, the excess oxygen is incorporated as isolated oxygen interstitials at low oxygen partial pressure, which cluster at higher oxygen concentration.[20–28] This leads to a variety of potential hydrogen traps. A further level of complexity is then due to the microstructure of polycrystalline oxide materials, which has an impact on the diffusivity of hydrogen,[17–19] as it does for the diffusivity of oxygen in fluorite oxides.[29–32]

Glascott proposed a comprehensive mathematical model for hydriding initiation in uranium metal, which included hydrogen diffusivity in the oxide coating layer.[33,34] However, such macroscopic modelling is unable to provide insight into the structural features that interact directly with hydrogen in the material. This can only be realised through atomistic modelling that can identify the geometry of hydrogen trapping sites.

[a]Department of Chemistry, University of Bath, Bath, BA2 7AY, UK. E-mail: s.c.parker@bath.ac.uk

[b]Department of Chemistry, University of Huddersfield, Queensgate, Huddersfield, HD1 3DH, UK. E-mail: m.molinari@hud.ac.uk

[c]AWE plc, Aldermaston, Reading, Berkshire, RG7 4PR, UK

[d]Interface Analysis Centre, University of Bristol, Bristol, BS2 8BS, UK

† Electronic supplementary information (ESI) available. See DOI: 10.1039/c8ta02817f

Recently, *ab initio* studies have begun to characterise the nature of hydrogen species, and have found that both hydroxyl groups and hydride species may form, with the latter identified as more favourable.[35,36] Other theoretical work has focussed on the adsorption, desorption and dissociation of water on uranium oxide surfaces,[37,38] which is one of the routes that hydrogen can be incorporated into the uranium oxide lattice and before reaching the metal. Whereas there is data suggesting the existence of hydrogen traps in oxygen-rich uranium oxide, there are no atom-level models to support this proposition. The present work applies *ab initio* modelling techniques to examine the dependence of hydrogen trapping on oxygen defect clusters under oxygen-rich conditions.

Methodology

First principle calculations

A cubic unit cell comprised of 32 UO_2 units was generated by a 2 × 2 × 2 expansion of the fluorite 4 UO_2 unit cell. All calculations were performed using the VASP code,[39] with PAW pseudopotentials and the GGA PBE functional.[40] The Dudarev[41] approach was used for the implementation of the onsite Hubbard U parameter, with $U = 4.5$ eV and $J = 0.54$ eV.[42] The plane-wave cut-off energy was set at 400 eV and a Γ-centred 2 × 2 × 2 Monkhorst–Pack k-point grid was used for all calculations, in line with previous work[22,25,43] and convergence criteria for the electronic and ionic relaxations were 1×10^{-6} eV per atom and 1×10^{-2} eV A^{-1}, respectively. All calculations were performed at constant pressure with collinear 1k antiferromagnetic ordering. This is considered an appropriate approximation for the experimentally observed 3k non-collinear antiferromagnetic ordering,[29,44] and is line with previous work.[22,25,26,28] VASP accounts for relativistic effects through scalar relativistic methods[45,46] and spin orbit coupling (SOC). In our previous work,[35] we examined the effect of SOC on hydrogen defects in UO_2. The produced a consistent shift in the energies, which is in line with previous work for UO_2.[47,48] SOC does not remove the tetragonal distortion caused by the antiferromagnetic ordering, which can only be removed using the experimentally observed 3k non-collinear ordering.[44] The effect of SOC has also been shown to be negligible on structure, relative stability and electronic properties of other actinide oxides.[49] For all these reasons and as the inclusion of SOC vastly increases the computational expense, it has not been included in here. All structural models were generated using the METADISE[50] code and all structural figures were created using VESTA.[51]

Results and discussion

UO_{2+x} structural models

The two smallest oxygen clusters proposed in uranium oxide are the split di-interstitial (I_2^x) and the 2 : 2 : 2 Willis cluster (W_{222}), shown in Fig. 1. We use the nomenclature common in the literature for the split interstitial clusters (I_2^x)[22] and have adapted this to also refer to the Willis clusters (W_{222}). Upon the incorporation of excess oxygen the UO_2 lattice is oxidised, such that for every additional oxygen, two uranium atoms are
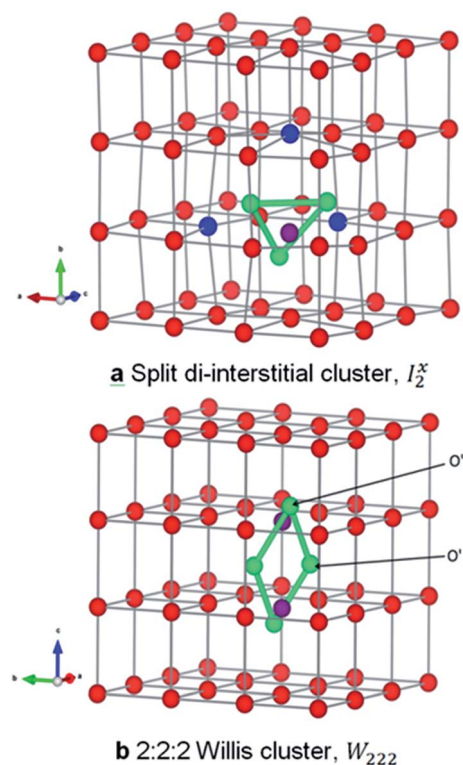

a Split di-interstitial cluster, I_2^x

b 2:2:2 Willis cluster, W_{222}

Fig. 1 Structure of oxygen defect clusters in UO_2. (a) Split di-interstitial (I_2^x) and (b) 2 : 2 : 2 Willis (W_{222}) clusters. Lattice oxygen shown in red. U^{4+}/U^{5+} are not shown for clarity. Oxygen interstitial (O_i'') shown in green. Significantly (>10%) displaced lattice oxygen shown in dark blue. Oxygen vacancies ($V_O^{\cdot\cdot}$) shown in purple. Bonds have been drawn in green to highlight defect cluster geometries.

oxidised from U^{4+} to U^{5+}. The Kroger–Vink notation is commonly used in the literature for defects in solids[22,26] and we use this to describe the point defects used as reference states.

A I_2^x cluster (Fig. 1a) has a central oxygen vacancy ($V_O^{\cdot\cdot}$) surrounded by three oxygen interstitials (O_i'') located approximately 1.6 Å away in $\langle 111 \rangle$ directions. This causes the displacement of three lattice oxygen by approximately 0.3 Å from their lattice sites, highlighted in blue in Fig. 1a. In the models presented here the excess oxygen changes the stoichiometry from $UO_{2.00}$ to $UO_{2.06}$, and leads to the oxidation of four nearest neighbour uranium ions to the cluster from U^{4+} to U^{5+}. A I_2^x cluster is found to have a formation energy of -123 kJ mol^{-1} in agreement with previously reported literature values.[22,23]

A W_{222} (Fig. 1b) consists of two $V_O^{\cdot\cdot}$ and four O_i'' each located approximately 1 Å from an octahedral interstitial site; two O_i'' are found in $\langle 110 \rangle$ directions (O′) and two in $\langle 111 \rangle$ directions (O″). The W_{222} cluster was the first defect cluster proposed to rationalise the UO_{2+x} structure,[20] and was initially predicted to be stable using interatomic potential model calculations.[21] However, the advent of DFT has demonstrated single, isolated W_{222} clusters are unstable with respect to I_2^x clusters.[23] Recently, DFT calculations have found that edge-sharing W_{222} clusters are stable in UO_{2+x}, but only in a narrow composition range ($0.125 < x < 0.25$),[25] becoming unstable by $x = 0.33$,[26]

This journal is © The Royal Society of Chemistry 2018

J. Mater. Chem. A, 2018, **6**, 11362–11369 | **11363**

emphasising how sensitive UO_2 defect chemistry is to oxygen partial pressure.

$UO_{2+x}H_y$ structural models

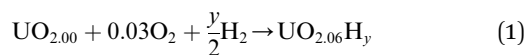Hydrogen was added to the $UO_{2.06}$ models of W_{222} (Willis cluster, Fig. 1b) and I_2^x (split di-interstitial cluster, Fig. 1a) clusters and the local hydrogen concentration was varied from 117 to 467 μg H/g UO_2, which is equivalent to y in $UO_{2+x}H_y$ varying from around 0.03 to 0.12. This is achieved by the addition of 1 to 4 hydrogen species to the oxygen clusters in simulation cell of $U_{32}O_{62+2}$. The addition of hydrogen to the oxygen clusters resulted in the formation of hydroxyl species within the cluster. As the defect clusters are made of oxygen and hydroxyl species these defect clusters will now collectively be referred to as oxy-hydroxyl clusters. The chosen configurations were selected to maximise the interactions between the oxygen and hydrogen species; details in the ESI.† The formation of each hydroxyl group within the oxygen defect split di-interstitial and Willis clusters (each containing $4U^{5+}$) results in the reduction of a U^{5+} to U^{4+}. The concentration of U^{5+} in each oxy-hydroxyl cluster is reported in ESI.†

It is important to note that, hydrogen can interact with oxygen clusters in different ways, and as we discuss later this drastically impacts the stability of the oxy-hydroxyl cluster. The newly formed hydroxyl group can hydrogen bond to lattice oxygen ions (L) or defect oxygen ions belonging to the cluster (D). This makes only two different conformations for each local hydrogen concentration in a I_2^x ($^LI_2^x$ and $^DI_2^x$), as it is composed of three equivalent O_i'' (Fig. 1a). The lower symmetry of the Willis cluster (arising from the two symmetrically inequivalent O_i'') is responsible for the greater number of possible distinct configurations; e.g. $^DW_{222}^{O',2O''}$ denotes three hydrogen atoms, one at a O' interstitial site and one at each of the two O'' sites, and all three species are hydrogen bonded oxygen species of the defect cluster (D).

Energetics of hydrogen in UO_{2+x}

In order to define irreversible and reversible hydrogen traps it is necessary to introduce two energy terms, the formation and the binding energies of oxy-hydroxyl clusters.

The formation of the oxy-hydroxyl clusters is considered as the energy of dissolving hydrogen and oxygen gas into a UO_2 matrix according to eqn (1).
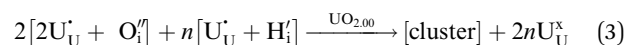
$$UO_{2.00} + 0.03O_2 + \frac{y}{2}H_2 \rightarrow UO_{2.06}H_y \quad (1)$$

with y taking values of 0.03, 0.06, 0.09 or 0.12, corresponding to 117, 234, 351 or 468 μg H/g UO_2, respectively. The thermodynamic stability of oxy-hydroxyl clusters is expressed using the formation energy (E_{Form}) of an oxy-hydroxyl defect cluster, normalised for the hydrogen concentration,

$$E_{Form} = \frac{E_{UO_{2.06}H_y} - \left(E_{UO_{2.00}} + \frac{y}{2}E_{H_2} + 0.03E_{O_2}\right)}{y} \quad (2)$$

where $E_{UO_{2.00}}$ and $E_{UO_{2.06}H_y}$ are the energies of stoichiometric $UO_{2.00}$ and hydrogen doped oxygen-rich $UO_{2.06}$, E_{H_2} and E_{O_2} are

the energies of molecular H_2 and O_2, respectively. A negative value of formation energy indicates that the oxy-hydroxyl cluster is stable.

In order to assess whether the oxy-hydroxyl clusters are more energetically favourable than isolated point defects, eqn (3) is considered, where the most stable isolated hydrogen defect is $[U_U^\bullet + H_i']$ comprising of a hole on the uranium as U^{5+} ($U_U^\bullet$) compensating the hydride ion (H_i'). The charge state of the hydrogen interstitial is dependent on the location in the lattice (Fig. 2), where the hydride is more stable than the protonic form by 26 kJ mol^{-1}. The isolated oxygen interstitial compensated by two U^{5+} is given by $[2U_U^\bullet + O_i'']$. These interstitial defects come together to form the oxy-hydroxyl defect cluster [cluster], either based on the split di-interstitial, I_2^x, $[(4 - n)U_U^\bullet + 3O_i'' + V_O^{\bullet\bullet} + nH_i^\bullet]$ or the $2 : 2 : 2$ Willis cluster, W_{222}, $[(4 - n)U_U^\bullet + 4O_i'' + 2V_O^{\bullet\bullet} + nH_i^\bullet]$, in the presence of hydrogen. In every case, hydrogen now forms protonic defects and so reduces the U^{5+} associated with the hydride to U^{4+} and reduces an additional U^{5+} associated with the O_i'', leading to the formation of the cluster in a simulation cell with a stoichiometry of $UO_{2.06}H_y$.

$$2[2U_U^\bullet + O_i''] + n[U_U^\bullet + H_i'] \xrightarrow{UO_{2.00}} [cluster] + 2nU_U^x \quad (3)$$

The preference for formation of oxy-hydroxyl clusters over isolated point defects (i.e. separated oxygen interstitial O_i'' and hydride) is expressed using the binding energy (E_{Bind}) of the oxy-hydroxyl cluster per hydrogen atom in the simulation cell, n,

$$E_{Bind} = \frac{E_{[cluster]} - \left(nE_{[U_U^\bullet + H_i']} + 2E_{[2U_U^\bullet + O_i'']}\right)}{n} \quad (4)$$

where each of the defect energies are defined as the difference in energy between the defective cell and the equivalent stoichiometric cell containing the same number of UO_2 formula
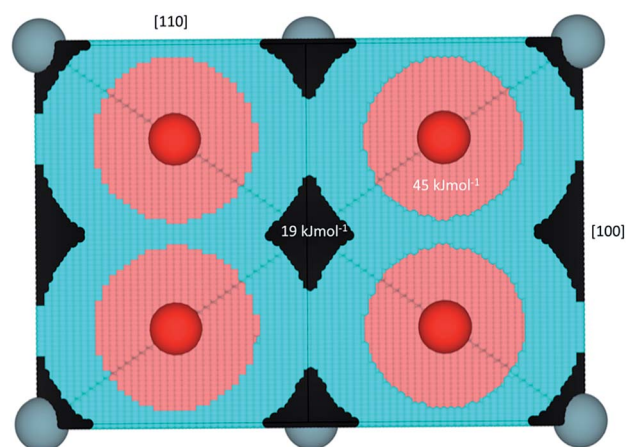

Fig. 2 Representation of hydrogen behaviour in UO_2 projected in a [110] direction. Black represents regions where hydride is predicted to be energetically most stable, light blue the $H^\bullet$ radical, pink protonic behaviour (i.e. forms a hydroxyl), red the lattice oxygen and blue are the uranium ions. The energies of formation for a hydride or hydroxyl defect by dissolving H_2 gas into UO_2 are shown on the respective regions. Values taken from ref. 35.

units, *e.g.* $E_{cluster} = E_{UO_{2.06}H_y} - E_{UO_2}$. The most stable isolated interstitial species within UO_2 for hydrogen (*i.e.* the hydride anion) and oxygen (*i.e.* an interstitial oxygen). For an isolated hydrogen ($E_{H_i'}$) this is a hydride ($E_{Form} = 19$ kJ mol^{-1}),[35] and an O_i'' in stoichiometric UO_2 ($E_{O_i''}$) for oxygen, with a formation energy calculated to be -119 kJ mol^{-1} in agreement with previous literature.[27] The reference energy for uranium oxide is the energy of stoichiometric UO_2. A negative value of binding energy indicates an energetic preference for the interstitial species to cluster in an oxy-hydroxyl defect cluster rather than form isolated point defects within the UO_2 lattice, *i.e.* hydride and O_i''. We follow the procedure of Minervini *et al.*[52] for calculating the binding energy.

The most stable oxy-hydroxyl $UO_{2+x}H_y$ clusters

The structures of the most stable configurations at each local hydrogen clusters at each local hydrogen concentration, 117 to 467 µg H/g UO_2, are presented in Fig. 3 along with their formation and binding energies. Data for all other configurations along with their energetics is presented in the ESI.† The most stable cluster is based on a I_2^x (split di-interstitial) geometry at local concentrations of 117 and 351 µg H/g UO_2, which correspond to 1 and 3 hydrogen species added to the oxygen cluster (-146 and -95 kJ mol^{-1}/H). This results in the reduction of $1U^{5+}$ to $1U^{4+}$ and $3U^{5+}$ to $3U^{4+}$ within the UO_2 lattice respectively, as the oxidised UO_{2+x} including a split di-interstitial cluster contains $4U^{5+}$. Whereas the most stable W_{222} (Willis) cluster is found at local concentrations of 234 µg H/g UO_2 and 467 µg H/g UO_2, which correspond to 2 and 4 hydrogen species added to the oxygen cluster (-119 and -76 kJ mol^{-1}/H), this is balanced by the reduction of $2U^{5+}$ at 234 µg H/g UO_2 and complete reduction of all U^{5+} at 467 µg H/g UO_2. In these clusters there is a strong interaction between the hydroxyl groups and lattice oxygen atoms. There seems to be an odd–even relationship for the most stable oxy-hydroxyl clusters. Oxygen clusters with odd numbers of interstitials oxygen atoms, the I_2^x, are stabilized by an odd number of hydrogen species, whereas oxygen clusters with even numbers of oxygen

interstitials (W_{222}) are stabilized by an even number of hydrogen species.

Energetics of oxy-hydroxyl $UO_{2+x}H_y$ clusters as a function of cluster geometry

Fig. 4 shows the formation (eqn (2)) and binding (eqn (4)) energies (in kJ mol^{-1}) per hydrogen species as a function of local hydrogen concentration ([H] in µg H/g UO_2) for the most stable configurations of the oxy-hydroxyl clusters. We provide separate figures depending on the nature of the oxygen cluster either split di-interstitial (I_2^x) or Willis (W_{222}) clusters, and whether the newly formed hydroxyl group hydrogen bonds to lattice oxygen ions (L) or defect oxygen ions belonging to the cluster (D). This gives four different combinations $^LI_2^x$, $^DI_2^x$, $^LW_{222}$ and $^DW_{222}$. In each case addition of hydrogen to the oxygen defect cluster resulted in favourable formation energies, however these become less favourable with increasing hydrogen concentration and the effect is less pronounced for $^DW_{222}$ (Fig. 4d). Additionally, oxy-hydroxyl clusters where a hydrogen bonding network is formed with lattice oxygen atoms (Fig. 4a and c) are always favoured compared to those with a hydrogen bonding network formed within the oxygen of the defect cluster (Fig. 4b and 3d). This shows a preference for the hydroxyl groups in the cluster to be arranged such that they hydrogen bond with oxygen of the lattice (L) rather than oxygen of the defect (D).

The preference for defect clusters over isolated point defects is expressed by the binding energy. This is generally unfavourable (*i.e.* isolated point defects dominate) at low hydrogen concentrations (117–234 µg H/g UO_2) and becomes increasingly favourable (*i.e.* defect clusters dominate) at higher concentrations (351–467 µg H/g UO_2). At the highest concentration (467 µg H/g UO_2) all clusters with favourable formation energies also have favourable binding energies (Fig. 4). There is no straightforward correlation between stability of the clusters and the total number of hydrogen bonds (Fig. 4). It appears that as the hydrogen concentration increases the number of hydrogen bonds per hydrogen decreases with the exception of $^LW_{222}$ clusters (Fig. 4c).
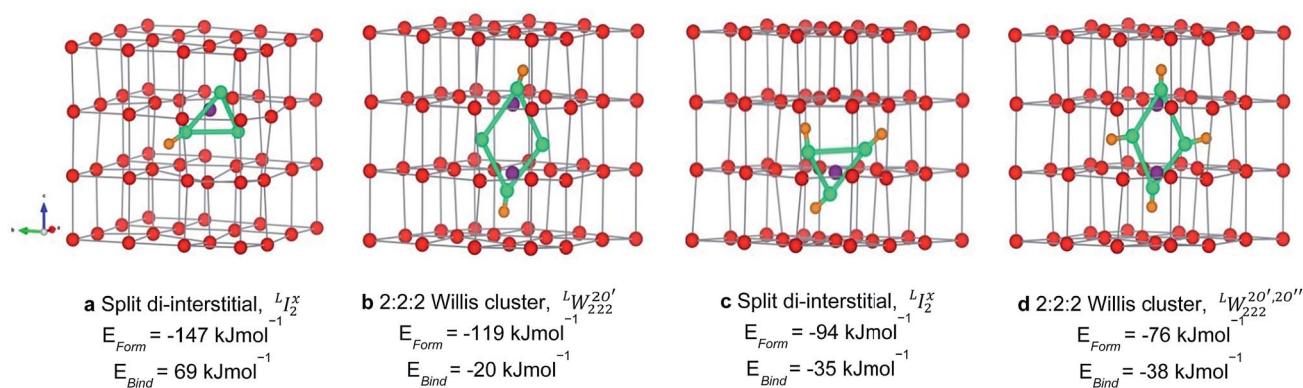

a Split di-interstitial, $^LI_2^x$
$E_{Form} = -147$ kJmol^{-1}
$E_{Bind} = 69$ kJmol^{-1}

b 2:2:2 Willis cluster, $^LW_{222}^{2O'}$
$E_{Form} = -119$ kJmol^{-1}
$E_{Bind} = -20$ kJmol^{-1}

c Split di-interstitial, $^LI_2^x$
$E_{Form} = -94$ kJmol^{-1}
$E_{Bind} = -35$ kJmol^{-1}

d 2:2:2 Willis cluster, $^LW_{222}^{2O',2O''}$
$E_{Form} = -76$ kJmol^{-1}
$E_{Bind} = -38$ kJmol^{-1}

Fig. 3 Structure of oxy-hydroxyl defect clusters in UO_2. Most stable defect clusters at (a) 117 µg H/g UO_2 (b) 234 µg H/g UO_2 (c) 351 µg H/g UO_2 (d) 468 µg H/g UO_2 local hydrogen concentration. Lattice oxygen shown in red. U^{4+}/U^{5+} not shown for clarity. Oxygen interstitial (O_i'') shown in green. Oxygen vacancies ($V_O^{\bullet\bullet}$) shown in purple. Hydrogen shown in orange. Bonds have been drawn in green to highlight defect cluster geometries. Formation and binding energies are given per hydrogen.

This journal is © The Royal Society of Chemistry 2018

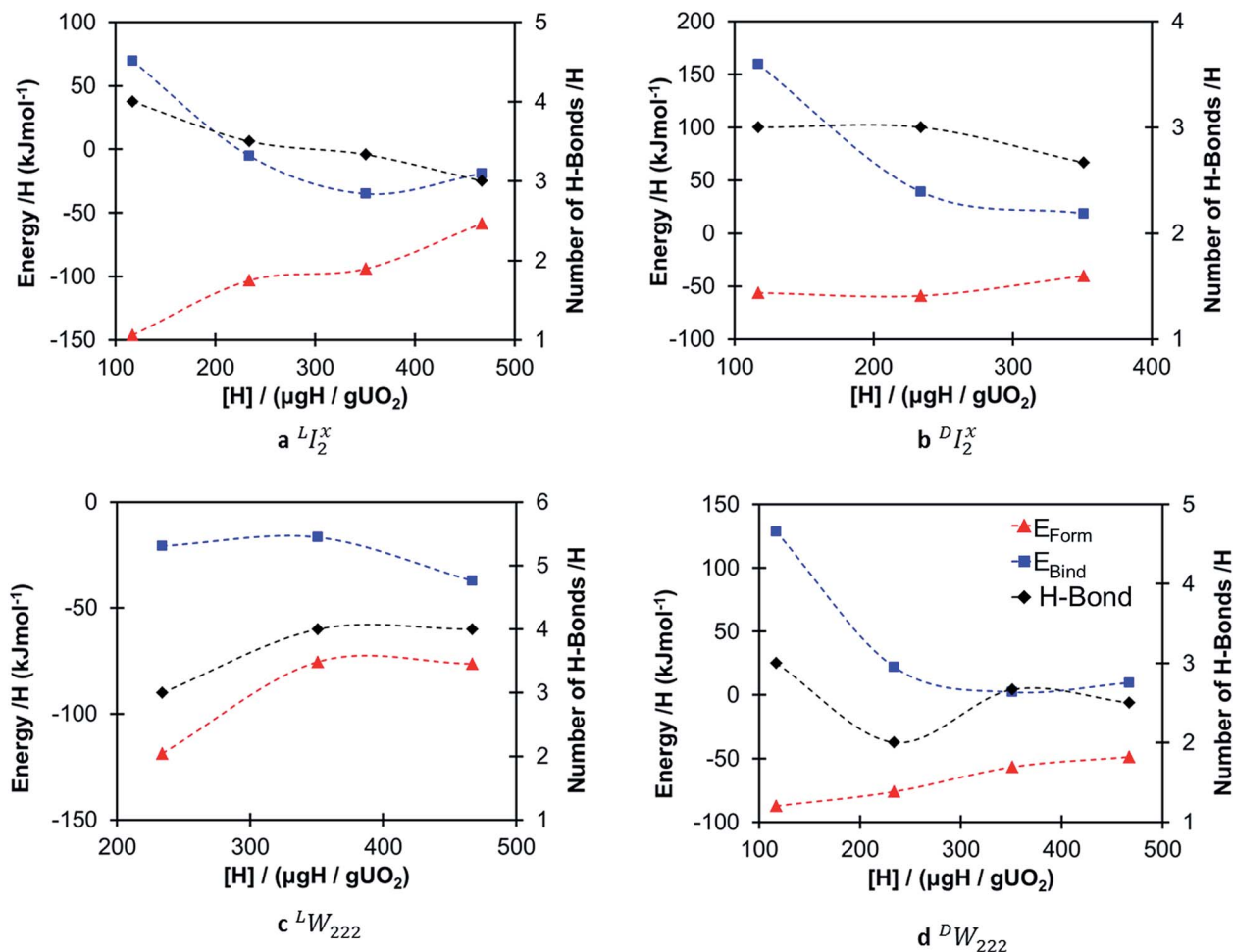*J. Mater. Chem. A*, 2018, **6**, 11362–11369 | **11365**

Fig. 4 Energetics of oxy-hydroxyl clusters. Formation energy (red triangles) and binding energy (blue squares) per hydrogen, and total number of hydrogen bonds (black diamonds) as a function of local hydrogen concentration for the most stable oxy-hydroxyl defect clusters.

We have investigated hydrogen interaction with two types of oxygen defect cluster (split di-interstitial (I_2^x) and 2 : 2 : 2 Willis (W_{222}) clusters) in uranium oxide. We found that the stability and geometry of these clusters radically change as a function of local hydrogen concentration. These oxygen defect clusters act as hydrogen traps and thus will macroscopically affect the material in terms of mechanical properties and hydrogen solubility and diffusion. This will significantly impact long term storage and disposal of uranium metal as hydrogen diffusion through the protective oxide layer forms pyrophoric hydride at the interfaces.

We found that, remarkably, the presence of hydrogen stabilises the Willis cluster when an appropriate hydrogen bonding network is established, suggesting that trapped hydrogen may have been present when these clusters were originally reported in uranium oxide.[20] Although the Willis cluster is stabilized by hydrogen, it is only the most stable defect at 234 and 467 µg H/g UO$_2$, with the split di-interstitial the most stable at 117 and 351 µg H/g UO$_2$. This indicates that oxygen defect chemistry in UO$_2$ is not only strongly dependent on oxygen stoichiometry,[25,26] but also on hydrogen partial pressure. This opens key chemical challenges to determine whether other

oxy-hydroxyl clusters will be directly stabilised, to what extent these clusters will appear in other materials, and whether the properties of oxide materials will be affected.

For all clusters, with one exception (ESI Table 4†), addition of hydrogen resulted in the formation of hydroxyl groups, which are essential for the formation of a hydrogen bonding network capable of stabilising oxy-hydroxyl clusters. Although there is little experimental work on the interaction of hydrogen with UO$_2$, hydroxyl groups were suggested as potential traps for hydrogen species by Wheeler[17] at concentrations of up to 10%. Sherman and Olander[19] also acknowledged the presence of hydrogen bound to a variety of defects (rather than simply dissolved as interstitial species) and proposed that oxygen vacancies may be a stable location for hydrogen defects. Indeed, our data shows that the Willis cluster can only be stabilized by forming a hydrogen bonding network that prevents an interstitial oxygen (O″) from moving to the vacant oxygen site (Fig. 1b) and thus relaxing to a I_2^x cluster. In some of the defect configurations, generally the least stable ones, we observe hydrogen species positioned at oxygen vacancy sites but still bound to an oxygen interstitial, which is in line with the proposition put forward by Sherman and Olander.[19]

11366 | J. Mater. Chem. A, 2018, 6, 11362–11369

This journal is © The Royal Society of Chemistry 2018

Based on the formation energies (which define the thermodynamic stability) and binding energies (which define the preference of having oxy-hydroxyl) we can identify, from a thermodynamic viewpoint, reversible and irreversible hydrogen traps in uranium oxide. This provides atom-level parameters that could be implemented in mathematical models to determine hydrogen transport in uranium oxide,[17,19,33,34] and each different hydrogen trap now may be considered explicitly. We suggest that oxy-hydroxyl clusters with favourable formation (*i.e.* negative) and binding energies (*i.e.* negative) correspond to irreversible traps, as they will form and will not dissociate into isolated defects. Clusters with a favourable formation energy and an unfavourable binding energy ($0 < E_{\text{Bind}} < 80$ kJ mol^{-1}) represent reversible hydrogen traps. These correspond to metastable intermediates that are reversible in nature, as the clusters can form but they are not the most stable defect configurations however they do not have sufficient energy for the hydroxyl bond to dissociate.[35] Whereas traps with a binding energy greater than the threshold of 80 kJ mol^{-1} are still metastable intermediates but are less likely to exist, as there is sufficient energy to convert the hydroxyl groups into hydride defects. This threshold for the binding energy of reversible traps (80 kJ mol^{-1}) corresponds to the energy barrier to form an isolated hydride group from a stable isolated hydroxyl species.[35]

Using our definition for the irreversible and reversible nature of hydrogen traps in UO$_2$, we have made an assessment of the probability of these oxy-hydroxyl clusters to be present within the lattice. This helps rationalise the experimentally observed reversible and irreversible hydrogen traps in UO$_2$, by providing atom level insights into the nature of defect clusters within UO$_2$. However, our calculations do not attempt to determine the absolute concentration of traps as this would require the calculation of free energy terms and is beyond the scope of this work, but represents a key area of future development. Furthermore, while the formation and binding energies allow us to define the nature of traps as reversible or irreversible, simply being an irreversible trap does not guarantee a high concentration of that trap. As in order for the cluster to have a greater concentration than the isolated point defects, its binding energy should be lower than the formation energy of the individual components.[53] Thus, a trap can be irreversible in nature and have a low concentration. Within the cluster configurations studied in this work, the only case where the binding energy is greater than the formation energies of the individual point defects is the $^{L}W_{222}^{2O',2O''}$ cluster (Fig. 3d), which suggests that this might be the dominant irreversible trap for hydrogen in UO$_2$.

We have generated thermodynamic distributions of irreversible and reversible hydrogen traps as a function of temperature, by calculating the probability of different clusters based on their formation energy. Eqn (5) displays the calculation of free energy, where the ΔG_i is the free energy for the oxy-hydroxyl cluster i, Ω is the degeneracy of the oxy-hydroxyl cluster (we report the degeneracy of a cluster in ESI†), $E_{\text{Form},i}$ is the formation energy calculated in eqn (2) and we rescale them so that this value to zero for the most stable defect cluster, R is the gas constant and T is the temperature.

$$\Delta G_i = \Omega e^{\left(\frac{-E_{\text{Form},i}}{RT}\right)} \tag{5}$$

The probability is then given by

$$P = \frac{\Delta G_i}{\sum_i \Delta G_i} \tag{6}$$

While this approach does not explicitly include the effect of temperature on the defect clusters, as the comparison is between defects all in the solid phase the cohesive energy term will be dominant and entropy terms are unlikely to reverse the conclusions. This again represents key areas for future research, both for the explicit inclusion of temperature and configurational entropy on the stability of defect clusters.

The thermodynamic distribution of all the clusters at each hydrogen concentration is presented in Fig. 5. The calculated probabilities show the predicted nature of the oxy-hydroxyl clusters based on the oxygen defect geometry (*i.e.* Willis or split di-interstitial) and trap nature (*i.e.* reversible or irreversible). As the concentration of hydrogen increases, there is a clear shift from reversible trapping, which dominates at the lowest concentration 117 μg H/g UO$_2$, to irreversible trapping, independent of cluster type (Fig. 5). Although we cannot compare our data directly with experimental de-trapping data,[17,19] as this accounts for kinetic parameters, it is intriguing that experimental data suggests that hydrogen dissolved in uranium oxide is not released by a diffusion controlled process. Examining the desorption curve for uranium oxide single crystal shows a first desorption peak at approximately 1100 K and a second and more discernible desorption peak at approximately 1700 K, associated with energies of 80 and 210 kJ mol^{-1} respectively.[19] This precludes hydrogen diffusion *via* interstitial sites in the UO$_2$ lattice and supports the idea that hydrogen is bound to discrete sites, as we see in our *ab initio* model structures. These hydrogen traps will be characterised by a binding energy and a rate constant of release.

While we calculated the binding energies for oxy-hydroxyl defect clusters in uranium oxide, we have no information on the rate constants for hydrogen release, which depend on temperature. When considering a thermodynamic distribution that accounts for all hydrogen traps at all local hydrogen concentrations (Fig. 6), irreversible trapping (*i.e.* negative binding energy) appears at temperatures higher than 900 K and is slightly more likely to be based on the Willis geometry (1.3% at 1000 K and 5% at 2000 K) compared to the split di-interstitial (0.3% at 1000 K and 3.5% at 2000 K). Up to 10% of irreversible hydrogen traps appear at 2000 K, whereas the majority (up to 90%) of hydrogen traps will still metastable intermediates (*i.e.* reversible traps) based on the I_2^x cluster (Fig. 6). As the irreversible traps are stabilised by a more complex hydrogen bonding network, they are more stable at higher local hydrogen concentrations and thus their thermodynamic distribution
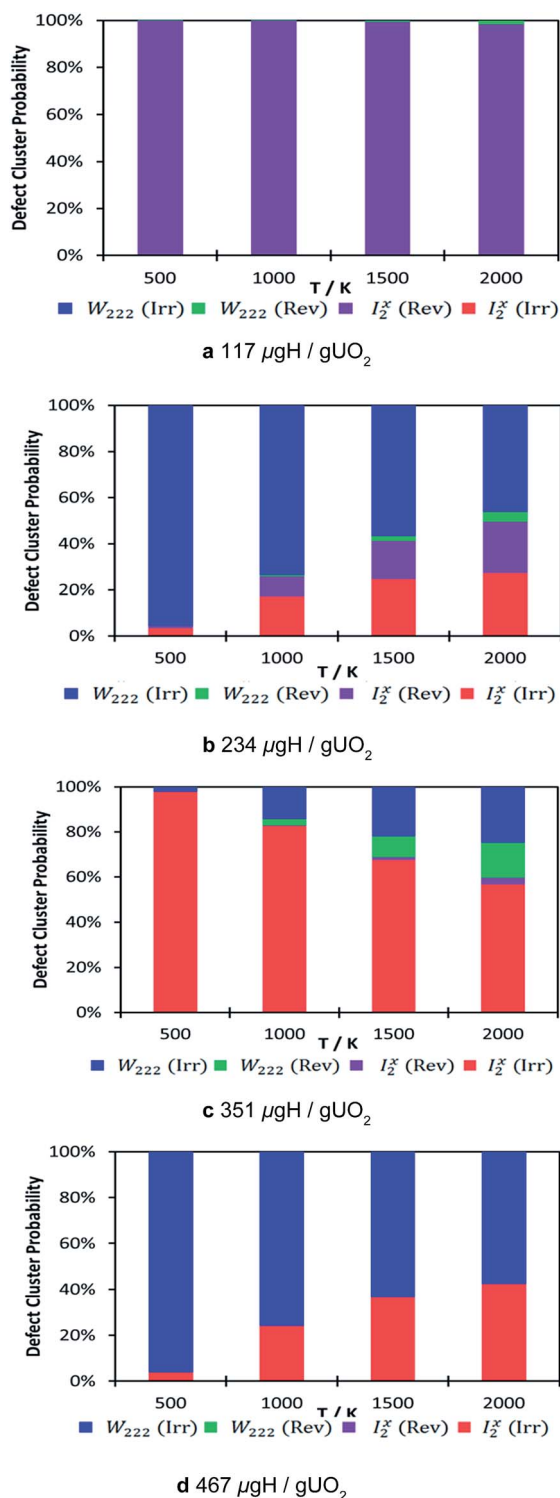
a 117 μgH / gUO$_2$

b 234 μgH / gUO$_2$

c 351 μgH / gUO$_2$

d 467 μgH / gUO$_2$

Fig. 5 Defect cluster probability at different local hydrogen concentrations as a function of temperature. The probability has been calculated relative to the most stable cluster for each local hydrogen concentration. Reversible W_{222} shown in green, irreversible W_{222} in blue, reversible I_2^x purple and irreversible I_2^x in red.

Fig. 6 Defect cluster probability as a function of temperature. The probability has been calculated relative to the most stable cluster for all concentrations. Reversible W_{222} shown in green, irreversible W_{222} in blue, reversible I_2^x purple and irreversible I_2^x in red.

Conclusions

To conclude, we found that hydrogen strongly affects the structure and energetics of oxygen defect clusters in uranium oxide, as has been shown for many other oxides.[1–5] Our analysis defines a thermodynamic route to determine reversible (metastable) and irreversible hydrogen traps, and show that there are stable local oxygen-rich regions (*i.e.* oxygen defect clusters) that can trap and sustain high local hydrogen concentrations despite low overall concentration in the sample. Our *ab initio* approach allows for quantitative measurement of the population of hydrogen traps, which changes as a function of local hydrogen concentration and temperature. This shows that we need atom-level models and insight if we are to predict macroscopic properties such as the dynamics of hydrogen defects and microstructural changes under non-equilibrium conditions that can arise in service due to the presence of extreme environments (*e.g.* radiation, temperature). Thus this work demonstrates when investigating defect clusters in oxides that the inclusion of hydrogen as part of these studies is overdue.

Conflicts of interest

There are no conflicts to declare.

Acknowledgements

increases with temperature, contrary to the metastable (reversible) traps that are mainly oxy-hydroxyl clusters with low local hydrogen concentration and a weaker hydrogen bonding network.
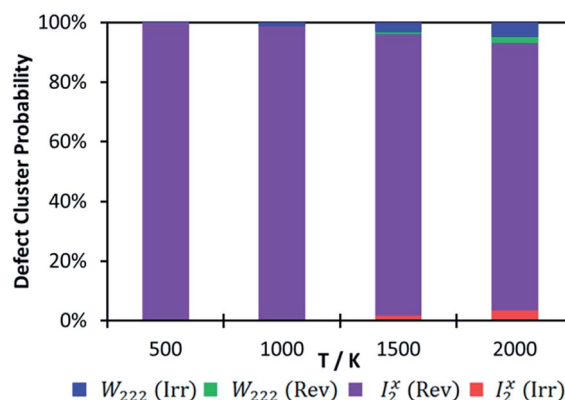
11368 | *J. Mater. Chem. A*, 2018, **6**, 11362–11369

This journal is © The Royal Society of Chemistry 2018

References

1 T. Norby, M. Widerøe, R. Glockner and Y. Larring, *Dalton Trans.*, 2004, 3012–3018.

2 T. Norby, *Nature*, 2001, **410**, 877878.

3 T. Norby and Y. Larring, *Curr. Opin. Solid State Mater. Sci.*, 1997, **2**, 593–599.

4 S. Ø. Stub, E. Vøllestad and T. Norby, *J. Phys. Chem. C*, 2017, **121**, 12817–12825.

5 L. Meng, X. De-Gang, M. Evan, L. Ju, Z. Xi-Xiang and S. Zhi-Wei, *Nat. Commun.*, 2016, **8**, 14564.

6 C. G. Van de Walle, *Phys. Rev. Lett.*, 2012, **85**, 10121015.

7 S. K. Cushing, F. Meng, J. Zhang, B. Ding, C. Chen, L. Ru-Shi, A. D. Bristow, J. Bright, P. Zheng and N. Wu, *ACS Catal.*, 2017, **7**, 1742–1748.

8 W. Xin-Ping and G. Xue-Qing, *Phys. Rev. Lett.*, 2016, **116**, 086102.

9 H. Malerød-Fjeld, D. Clark, I. Yuste-Tirados, R. Zanon, D. Catalan-Martinez, D. Beeaff, S. H. Morejudo, P. K. Vestre, T. Norby, R. Haugsrud, J. M. Serra and C. Kjølseth, *Nat. Energy*, 2017, **2**, 923–931.

10 E. L. Silva, A. G. Marinopoulos, R. B. L. Vieira, R. C. Valao, H. V. Alberto, J. M. Gil, R. L. Lichti, P. W. Mengyan and B. B. Baker, *Phys. Rev. B*, 2016, **94**, 014104.

11 X. Leng, J. Pereiro, J. Strle, G. Dubuis, A. T. Bollinger, A. Gozer, J. Wu, N. Litombe, C. Pangopoulos and C. I. BoZovi, *npj Quantum Materials*, 2017, **2**, 1–7.

12 A. Borgschulte, O. Sambalova, R. Delmelle, S. Jenatsch, R. Hany and F. Nuesch, *Sci. Rep.*, 2017, **7**, 40761.

13 C. A. Colmenares, *Prog. Solid State Chem.*, 1984, **15**, 257–364.

14 A. G. Ritchie, *J. Less-Common Met.*, 1984, **98**, 193–214.

15 J. M. Haschke, T. H. Allen and L. A. Morales, *J. Alloys Compd.*, 2001, **314**, 78–91.

16 C. A. Stitt, N. J. Harker, K. R. Hallam, C. Paraskevoulakpos, A. Banos, S. Rennie, J. Jowset and T. B. Scott, *PLoS One*, 2015, **10**, 1–13.

17 V. J. Wheeler, *J. Nucl. Mater.*, 1971, **40**, 189–194.

18 D. R. Olander, D. Sherman and M. Balooch, *J. Nucl. Mater.*, 1982, **107**, 31–45.

19 D. F. Sherman and D. R. Olander, Hydrogen dissolution in and release form nonmetals I uranium dioxide, *J. Nucl. Mater.*, 1989, **166**, 307–320.

20 B. T. M. Willis, *Nature*, 1963, **197**, 755–756.

21 C. R. A. Catlow, *Proc. R. Soc. London*, 1977, **353**, 533–561.

22 D. A. Andersson, J. Lezama, B. P. Uberuaga, C. Deo and S. D. Conradson, *Phys. Rev. B*, 2009, **79**, 024110.

23 H. Geng, Y. Chen, Y. Kaneta, M. Iwasawa, T. Ohnuma and M. Kinoshita, *Phys. Rev. B: Condens. Matter Mater. Phys.*, 2008, **77**, 104120.

24 J. Wang, R. C. Ewing and U. Becker, *Sci. Rep.*, 2014, **4**, 4216.

25 N. A. Brincat, M. Molinari, S. C. Parker, G. C. Allen and M. T. Storr, *J. Nucl. Mater.*, 2015, **456**, 329–333.

26 N. A. Brincat, M. Molinari, G. C. Allen, M. T. Storr and S. C. Parker, *J. Nucl. Mater.*, 2015, **467**, 724–729.

27 F. Gupta, G. Brillant and A. Pasturel, *Philos. Mag.*, 2007, **87**, 2561–2569.

28 L. Desgranges, G. Baldinozzi, D. Simeone and H. E. Fischer, *Inorg. Chem.*, 2016, **55**, 7485–7491.

29 B. Dorado, G. Jomard, M. Freyss and M. Bertolus, *Phys. Rev. B: Condens. Matter Mater. Phys.*, 2010, **82**, 035114.

30 S. T. Murphy, E. E. Jay and R. W. Grimes, *J. Nucl. Mater.*, 2014, **447**, 143–149.

31 N. R. Williams, M. Molinari, S. C. Parker and M. T. Storr, *J. Nucl. Mater.*, 2015, **458**, 45–55.

32 L. Sun, D. Marrocchelli and B. Yildiz, *Nat. Commun.*, 2015, **6**, 6294.

33 J. Glascott, *Philos. Mag.*, 2014, **94**, 221–241.

34 J. Glascott, *Philos. Mag.*, 2014, **94**, 1393–1413.

35 J. M. Flitcroft, N. A. Brincat, M. Molinari, S. C. Parker and M. T. Storr, *Chem. Commun.*, 2015, **51**, 16209.

36 A. Bingyun, Q. Ruizhi, L. Haiyan and C. Piheng, *J. Phys. Chem. C*, 2016, **120**, 18445–18451.

37 T. Bo, J. Lan, Y. Zhao, C. He, Z. Chai and W. Shi, *J. Nucl. Mater.*, 2014, **54**, 446–454.

38 B. E. Tegner, M. Molinari, A. Kerridge, S. C. Parker and N. Kaltsoyannis, *J. Phys. Chem. C*, 2016, **121**, 1675–1682.

39 G. Kresse and J. Furthmuller, *Phys. Rev. B: Condens. Matter Mater. Phys.*, 1996, **54**, 11169–11186.

40 J. P. Perdew, K. Burke and M. Ernzerhof, *Phys. Rev. Lett.*, 1996, **77**, 3865–3868.

41 M. R. Castell, S. L. Dudarev, C. Muggelberg, A. P. Sutton, G. A. A. D. Briggs and D. T. Goddard, *J. Vac. Sci. Technol.*, 1998, **16**, 1055.

42 T. Yamazaki and A. Kotani, *J. Phys. Soc. Jpn.*, 1991, **60**, 49–52.

43 N. A. Brincat, S. C. Parker, M. Molinari, G. C. Allen and M. T. Storr, *Inorg. Chem.*, 2014, **53**, 12253–12264.

44 R. Laskowski, G. K. H. Madsen, P. Blaha and K. Schwarz, *Phys. Rev. B: Condens. Matter Mater. Phys.*, 2004, **69**, 140408.

45 L. Kleinman, *Phys. Rev. B: Condens. Matter Mater. Phys.*, 1980, **21**, 2631.

46 A. H. MacDonald, W. E. Pickett and D. D. Koelling, *J. Phys. Chem. C*, 1980, **13**, 2675–2683.

47 F. Bottin, G. Geneste and G. Jomard, *Phys. Rev. B: Condens. Matter Mater. Phys.*, 2016, **93**, 115438.

48 P. Santini, R. Lemanski and P. Edros, *Adv. Phys.*, 1999, **48**, 537–653.

49 X. D. Wen, R. L. Martin, L. E. Roy, G. E. Scuseria, S. P. Rudin, E. R. Batista, T. M. McCleskey, B. L. Scott, B. Bauer, J. J. Joyce and T. Durakiewicz, *J. Chem. Phys.*, 2012, **137**, 154707.

50 G. W. Watson, E. T. Kelsey, N. H. deLeeuw, D. J. Harris and S. C. Parker, *J. Chem. Soc., Faraday Trans.*, 1996, **92**, 433–438.

51 K. Momma and F. Izumi, *J. Appl. Crystallogr.*, 2008, **41**, 653–658.

52 L. Minervini, M. O. Zacate and R. W. Frimes, *Solid State Ionics*, 1999, **116**, 339–349.

53 C. G. Van de Walle and J. Neugebauer, *J. Appl. Phys.*, 2004, **91**, 3851–3879.

This journal is © The Royal Society of Chemistry 2018

J. Mater. Chem. A, 2018, **6**, 11362–11369 | **11369**